Establishment of human glioblastoma cell culture collection

Hélèna L. Denis[1,2*], Jaëlle Méroné[1,2,3*], Valérie Watters[1,3], Victoire Fort[1,3], Gabriel Khelifi[1,3], Mikalie Lavoie[1,3], Line Berthiaume[1,4], Félix Rondeau[1,3], Émy Beaumont[1,3], Karine Michaud[5], Myreille D'Astous[5], Stephan Saikali[6], Marc-Étienne Huot[1,3,6], Étienne Audet-Walsh[1,4,7#], Maxime Richer[1,2,6#], Samer M.I. Hussein[1,3,6#]

1. Université Laval, Québec, QC, Canada;
2. Axe neurosciences du Centre de recherche du Centre hospitalier universitaire (CHU) de Québec-Université Laval, Québec, QC, Canada;
3. Axe oncologie du Centre de recherche du CHU de Québec-Université Laval, Québec, QC, Canada;
4. Axe endocrinologie et néphrologie du Centre de recherche du CHU de Québec-Université Laval, Québec, QC, Canada;
5. Department of Surgery, CHU de Québec-Université Laval, Québec, QC, Canada;
6. Department of Molecular Biology, Biochemistry and Pathology, CHU de Québec, Université Laval, Québec, QC, Canada;
7. Department of Molecular Medicine, CHU de Québec, Université Laval, Québec, QC, Canada.

** equal contribution*

#Co-Correspondence:

Étienne Audet-Walsh, Ph.D.
Department of Molecular Medicine
Axe Endocrinologie - CRCHU de Québec – Université Laval
CHUL – Pavillon R
2705 boulevard Laurier, Québec, QC, Canada G1V 4G2
E-mail: Etienne.Audet-Walsh@crchudequebec.ulaval.ca

Maxime Richer, MD, PhD FRCPC (Neuropathology)
Department of Molecular Biology, Medical Biochemistry, and Pathology
Axe neurosciences - CRCHU de Québec – Université Laval
CHUL – Pavillon T
2705 boulevard Laurier, Québec, QC, Canada G1V 4G2
E-mail: maxime.richer@crchudequebec.ulaval.ca

Samer M. I. Hussein, Ph.D
Department of Molecular Biology, Medical Biochemistry, and Pathology
Université Laval Cancer Research Centre
Oncology division - CRCHU de Québec – Université Laval
Hôpital de l'Enfant-Jésus - Pavillon L
1401, 18e Rue, Québec (Québec) G1J 1Z4
Email: samer.hussein@fmed.ulaval.ca

ABSTRACT

Background/Objectives: Glioblastoma (GBM) is the most aggressive type of primary brain cancer, affecting children and adults alike and is associated with a poor prognosis (less than 15 months). It is therefore critical to develop more effective therapies that improve survival and reduce side effects for these lethal brain cancers. Glioblastoma cells constantly reprogram their metabolism to adapt to changing conditions. As current treatments are not effective, the need for a deeper understanding of metabolic processes and signaling pathways grows critical.

Methods: To support this, we have established a collection of human GBM cell cultures derived from freshly resected tumor tissues from 78 patients undergoing surgery at CHU de Québec – Université Laval. We aimed to characterize this cell lines by combining histologic, metabolomic and gene expression analysis.

Results: Among the 21 cases that successfully generated cell lines, all were IDH-wildtype (IDH-wt) GBMs, with molecular profiles, including Ki-67 proliferation index, ATRX status, p53 expression, and MGMT promoter methylation. Characterization of five cell lines revealed significant metabolic and phenotypic heterogeneity, with differences in amino acid levels, TCA cycle metabolites, and RNA expression of GBM subtype markers. Our data suggest that mesenchymal-like GBM cells exhibit higher metabolic activity compared to proneural-like cells.

Conclusions: Together, the analyses highlight the heterogeneity of GBM cells across patients. These findings emphasize the complexity of GBM and the need for personalized approaches in treatment, taking into account the diverse metabolic and molecular characteristics of GBM cells.

Keywords: human glioblastoma stem cells, biobank, metabolome, gene expression.

INTRODUCTION

Gliomas, glioneuronal tumors, and neuronal tumors represent the most frequent and diverse tumors affecting the central nervous system (CNS)[1]. According to the fifth edition of the World Health Organization classification of CNS tumors[2], they are divided into six distinct groups: (1) Adult-type diffuse gliomas include glioblastoma (IDH-wildtype), astrocytoma (IDH-mutant), and oligodendroglioma (IDH-mutant and 1p/19q-codeleted), which are commonly encountered in adult neuro-oncology practice; (2) Pediatric-type diffuse low-grade gliomas are typically associated with a favorable prognosis; (3) Pediatric-type diffuse high-grade gliomas are generally more aggressive; (4) Circumscribed astrocytic gliomas are characterized by a more localized growth pattern compared to the infiltrating nature of adult-type diffuse and pediatric-type diffuse high-grade gliomas; (5) Glioneuronal and neuronal tumors, a diverse group often exhibiting neuronal differentiation, along with (6) ependymal tumors, represent the remaining categories in the classification.

Among adult-type diffuse gliomas, IDH-wildtype (wt) glioblastoma (GBM) are the most common and aggressive primary brain tumors in adults[1]. Their highly infiltrative and recurrent nature leads to failures following chemotherapy and radiotherapy, as well as a short median survival (less than 15 months)[3]. There is an urgent need to develop new therapies to improve the survival and quality of life of individuals affected by GBM. IDH-wt GBM exhibits molecular heterogeneity, evident not only between different tumors (intertumoral heterogeneity) but also within the same tumor (intratumoral heterogeneity). This variability reflects the diversity in its histological and molecular characteristics, cellular origins, topographical variations, growth patterns, and therapy sensitivities, all contributing to its aggressive behavior and poor prognosis. Key molecular alterations in GBM include TERT promoter mutations, EGFR gene amplification, and the combined gain of chromosome 7 and loss of chromosome 10 (+7/−10)[2]. Comprehensive transcriptomic analyses further delineated this heterogeneity, identifying molecular signatures that categorize various adult-type GBM subtypes such as classical, mesenchymal, and proneural[4–6]. Single-cell transcriptomic data subsequently revealed diverse cellular states within a single tumor, including neural progenitor-like (NPC-like), oligodendrocyte progenitor-like (OPC-like), astrocyte-like, and mesenchymal-like (MES-like) states, each driven by specific genetic alterations and influenced by the microenvironment and treatments[7,8].

Additionally, the metabolism of glioblastoma also shows significant heterogeneity and plasticity. While these cells primarily use glucose as their main metabolic fuel, they can also utilize other

substrates depending on their genetic makeup and environmental conditions. These include amino acids such as glutamine and glutamate, lipids like fatty acids and lipid droplets, and other sources such as acetate[9]. The robust proliferative activity of cancer cells demands a high supply of energy (ATP), precursors for macromolecules (carbohydrates, lipids, proteins, and nucleic acids), and reducing equivalents to support their rapid growth and survival. Furthermore, these cells continuously reprogram their metabolism to adapt to ever-changing environmental conditions[10].

Given the limited success of traditional cancer therapies targeting mechanisms such as growth, cell cycle regulation, autophagy, DNA repair, apoptosis, angiogenesis, and immune checkpoints, it is increasingly crucial to advance our understanding of oncogenic metabolic mechanisms and their associated signaling pathways. This advancement is essential for identifying novel therapeutic targets and subsequently developing innovative treatment strategies[11–13]. To further this research, it is crucial to perform comprehensive transcriptomic (coding and non-coding) and metabolomic characterizations of GBM cell-based models that closely mimic the complex biology and molecular subtypes of GBM. There is also a strong need for more accurate cell models of GBM, as widely used lines like U87 and U251, have limitations. These commercial cell lines, while historically important, are altered by serum-containing culture media, leading to genetic and transcriptomic changes. Additionally, tumors formed from these lines in mouse models fail to replicate key GBM features, and the lack of clinical characterization of the original patient tumors further limits their relevance to patient conditions[14]. While sequencing data from GBM tissues and cell lines have been extensively shared, there are only a few and recent databases that include both tissues and cell lines along with matched normal samples[15–18]. In alignment with this goal, we have established a collection of human GBM cell cultures derived from freshly resected tumor tissues from patients undergoing surgery at CHU de Québec – Université Laval. Culturing these cells under conditions that preserve glioma stem cells (GSCs) is particularly important as GSCs are thought to drive recurrence and therapy resistance due to their unique capabilities for growth, progression, and resilience against treatments[19–21].

MATERIALS AND METHODS

Ethics statement and participant recruitment

To create our human GBM cell culture resource, freshly resected tumor tissues were collected from patients undergoing surgery at the CHU de Québec – Université Laval, Hôpital de l'Enfant-Jésus. The institutional review board (#2023-6392) approved the study in accordance with the Declaration of Helsinki, and all participants provided written informed consent. Our clinical pathological facilities at CRCHU de Québec provided results for: 1) loss of 10q chromosome, assessed by PTEN loss, and amplification of EGFR using FISH, and 2) p53, IDH and ATRX presence or absence of mutation through immunohistochemistry.

Cell culture media

GBM media: NeuroCult™ NS-A Basal Medium (StemCell Technologies, #05750) supplemented with 2 µg/mL Heparin (Sigma, #H3393), 10 ng/mL FGF2 (PeproTech, #100-18B), 20 ng/mL EGF (PeproTech #AF-100-15) and 1µM CHiR (Cedarlane Labs, #S2924).

DMEM-F12 media: DMEM/F-12, HEPES (Thermofisher Scientific Gibco™, #11330057) supplemented with 20mM of GlutaMAX™ Supplement (Thermofisher Scientific Gibco™, #35050061) 1x of MEM Non-Essential Amino Acids Solution (Thermofisher Scientific Gibco™, #11140050), 1mM of Sodium Pyruvate (Thermofisher Scientific Gibco™, #1360070), 0.11 mM of 2-Mercaptoethanol (Thermofisher Scientific Gibco™, #21985023), 40mg/mL of human recombinant Insulin (Thermofisher Scientific Gibco™, #12585014) and 1x of N2 (100x, homemade and composed of progesterone (6 mg/mL), putrescine dihydrochloride (160 mg/mL), Sodium selenite 30 mM, apo-Transferrin human (100 mg/mL).

Neurobasal media: Neurobasal™ Medium Catalog (Thermofisher Scientific Gibco™, #21103049) supplemented with 20mM GlutaMAX™ Supplement (Thermofisher Scientific Gibco™, #35050061), 1x of MEM Non-Essential Amino Acids Solution (Thermofisher Scientific Gibco™, #11140050) and 1x of B-27™ Supplement (Thermofisher Scientific Gibco™, #17504044).

Neurosphere media: 2 portions of DMEM-F12 media for 1 portion of Neurobasal media supplemented with 500 ng/mL Heparin (Sigma, #H3393), 20 ng/mL FGF2 (PeproTech, #100-18B) and 20 ng/mL EGF (PeproTech #AF-100-15).

Preparation of GBM cell lines

The biopsy was divided into three fragments (**Figure 1A**). One fragment was flash-frozen and stored in liquid nitrogen, while another was formalin-fixed and paraffin-embedded. The last fragment was processed under sterile conditions to establish a GBM cell line through the following steps. First, we washed the biopsy with DPBS (Fisher Scientific, #14190250), then finely chopped it with a scalpel. Next, enzymatic dissociation was performed at 37°C for 10 minutes using TrypLETM enzyme (Thermofisher Scientific Gibco™, #12604013). To neutralize the enzyme, three volumes of DMEM (Thermofisher Scientific Gibco™, #11965118) supplemented with 5% KnockOut™ Serum Replacement (Thermofisher Scientific Gibco™, #A318502) was added. After a centrifugation at 1000 RPM for 4 minutes, cells were pelleted, and supernatant was trashed. GBM media was then added to the tube, and the pellet was dissociated with ten up-and-down pipettings, followed by another centrifugation at 300 RPM for 2 minutes. Both the supernatant and the pellet were placed separately into wells of a 6-well ultra-low adherence plate (Fisher Scientific, #07-200-602) with GBM media supplemented with 1x penicillin-streptomycin (Fisher Scientific, #15140148), incubating them at 37°C with 5% CO2. After a few weeks, neurospheres formed in suspension, contingent upon the presence of glioblastoma stem cells (GSCs) in the GBM biopsy. Finally, neurospheres were dissociated and cultured as monolayers in GBM medium without antibiotics, using wells coated with GeltrexTM (Gibco, #A14133).

Limited dilution assay

On the day of the experiment, cells were seeded in an ultra-low attachment 96-well plate (Fisher Scientific Corning™ Costar™, #07-200-603) filled with *Neurosphere* media. The plate was divided into four sections, each containing 24 wells with 3, 10, 30, or 1000 cells. After seven days, the number of negative wells were counted under a microscope. A negative well was defined as a well with no neurosphere formation. The experiment was performed in duplicate. By plotting the percentage of wells without neurospheres against the log of the number of cells deposited per well (3, 10, 30, 100), we generated a linear regression ($y = ax + b$). When plating at limiting dilutions, the proportion of culture wells with no neurospheres (negative wells) follows the zero term of the Poisson distribution: $F0 = e\text{-}x$. The number of cells needed to isolate one stem cell ($x = 1$) is calculated using $F0 = e(-1) = 0.37$ or 37%. The percentage of GSC cells was assessed using the following formula: $\% \text{ GSCs} = (a/(\ln(37) - b)) * 100$.

Metabolomic assay

For metabolomics, cells were processed using a standardized protocol[22,23]. In brief, after being passaged, each primary cell line was seeded in two 10-cm dishes. Two days later, samples of about 1,000,000 cells were harvested for metabolomics. To this end, cells were rinsed twice with ice-cold saline (NaCl 0.9%) on ice. After the second wash, cells were harvested in dry ice-cold 80% methanol and stored at -80ºC. On the day of analysis, samples were extracted by sonication in ice-cold water before being derivatized by methoxymation and silylation. Samples were then analyzed using an Agilent 8890 GC with a DB5-MS + DG capillary column coupled to an Agilent 5977B MS using electron impact ionization (EI) at 70 eV (Agilent Technologies, Santa Clara, CA, USA). Finally, the Agilent MassHunter Workstation software was used for analysis and specific metabolites were identified using the NIST/EPA/NIH mass spectra library (NIST, Gaithersburg, MD, USA).

RT-qPCR

Total RNA from cell pellets was collected using QIAshredder columns (QIAGEN, #79656) and the EZ-10 kit (Bio-basic, #BS88583). 2500 ng of RNA was treated with DNase (Thermo Fisher Scientific, #EN0521), and then 500 ng of treated RNA was reverse transcribed into cDNA using the iScript gDNA clear cDNA synthesis kit (Bio-Rad, #1725035). cDNA was quantified using the fluorescent probe SYBR-green (Applied Biosystems, #4472908), and qPCR was performed in triplicate. A pool of non-reverse transcribed RNA from each line served as a control sample. For RT-qPCR analysis, the relative expression of each gene was calculated in GBM lines using the delta Cq method. RPL27 was used as the housekeeping gene. A list of ARN targets is available in **Table 1**.

Statistical analyses

The D'Agostino & Pearson test was used to determine normality. When comparing two groups, Unpaired t-test was performed. In case data did not reached normality, a Mann-Whitney test was used. When comparing more than two groups, one-way ANOVA followed by Tukey's multiple comparison test was performed. When data did not meet the assumption of normality, the nonparametric Kruskal-Wallis test was used to compare groups, followed by Dunn's post-hoc test. In figures representing pairwise comparisons, data are expressed as means ± standard error of the mean (SEM). All statistical analyses above were performed using GraphPad Prism 10.1.2 (GraphPad Software Inc., San Diego, CA, USA) or JMP Pro 17 (JMP Statistical Discovery LLC,

Cary, NC, USA). Results were considered statistically significant when the p-value was less than 0.05.

RESULTS

Human glioblastoma cell culture collection

GBM resection specimens were collected, and each sample was divided into three distinct pieces (**Figure 1A**). The first piece was flash-frozen to preserve the molecular integrity of the tissue. The second piece was processed into formalin-fixed, paraffin-embedded (FFPE) blocks for histopathological and molecular analyses. The third piece underwent mechanical and enzymatic dissociation to isolate single cells. These cells were subsequently cultured under optimized conditions for several weeks to establish patient-derived GBM cell lines. The initial cohort comprised 78 patients with IDH-wt GBM, including 34 women and 44 men, with median ages of 60 and 59 years, respectively (**Figure 1B-C**). The majority of cases (83%) were derived from initial resections performed at the time of primary diagnosis, prior to the administration of any treatment. The cohort included a higher number of patients with IDH-wt status (77%), this percentage is close to the incidence observed in the literature, which is 80% in the US[24]. As expected [2], the Ki-67 proliferative index was higher in IDH-wt GBM (**Figure 1D**), with ATRX status aligning accordingly (83% vs 17%; **Figure 1E**). Additionally, 61% of tumors exhibited p53 overexpression, suggestive of a TP53 gene mutation. Notably, p53 overexpression was identified in 36% of IDH-wt cases compared to only 50% of IDH-mutated cases. MGMT promoter hypermethylation was observed in 54%. IDH-mutated biopsies were not tested for MGMT status.

Establishment and Characterization of Patient-Derived GBM Cell Lines

The initial cohort was representative in terms of age, gender, and the distribution of molecular alterations, with no evidence of selection bias. Among the 21 cases that successfully generated cell lines, there were 8 women and 13 men, with median ages of 65 and 58 years, respectively (**Figure 2A-B**). Of these, 18 cases originated from primary resections (**Figure 2C**). As expected, all GBMs cell lines were IDH-wt, with an average Ki67 index of 30% and ATRX-wt status (**Figure 2D-E**). The distribution of p53 status was 64% WT and 36% Mut, while MGMT promoter methylation was 48% WT vs 52% Met (**Figure 2E**). We then focused on characterizing the newly isolated GBM cell line, working initially on 9 individual lines (**Figure 2F**). Morphology varies between these lines with most showing a fibrillary morphology in the adherent state, as expected from astrocytic-like cells. A limiting dilution assay, used to evaluate the self-renewal and proliferative capacity of GSCs, revealed significant variability, with GSC percentages ranging from 4.5% to 26% (**Figure 2F**). Among the 5 selected cell lines, fluorescence in situ hybridization (FISH)

studies identified EGFR amplification in two lines (C14, C19) and loss of chromosome 10q in two others (C15, C39). The latter is typically associated with the loss of the tumor suppressor PTEN, a key driver of PI3K/AKT pathway activation, contributing to tumor growth and resistance to apoptosis. No correlations were observed between GSC percentage and factors such as sex, p53 status, MGMT status, EGFR amplification, or loss of chromosome 10q (**Figure 2F**).

Next, five cell lines were characterized based on their metabolite levels (**Figure 3A-B**). Our targeted metabolomic profiling included essential and non-essential amino acids, as well as intermediates of bioenergetic pathways such as the TCA cycle. The five cell lines demonstrated substantial heterogeneity in their metabolic profiles. C38 exhibited the highest levels of essential and non-essential amino acids, such as leucine and glutamine, along with elevated levels of TCA cycle metabolites, including citrate and fumarate. C15, C19, and C39 displayed intermediate levels of most metabolites; however, certain metabolites, such as lysine and cysteine, were as elevated as those in C38. In contrast, C14 exhibited high levels of glycine, serine, and succinate but had the lowest levels of most other metabolites, indicating distinct metabolic activity in this cell line.

To further characterize these cell lines, we performed RT-qPCR to evaluate the relative expression of specific markers for mesenchymal-like (CD44), mesenchymal-transition (TGFB1 and SNAI2), NPC-like (DLL3), and OPC-like (Olig2) GBM subtypes[7,8,25,26]. The expression of GBM subtype markers also showed variability across the cell lines (**Figure 3C**). Notably, CD44 was expressed in C15, C19, and C38 but was undetectable in C14 and C39. TGFB1 expression was significantly higher in C19 compared to the other cell lines. SNAI2 levels were slightly elevated in C19, C38, and C39 relative to C14 and C15. DLL3 and Olig2 were exclusively expressed in C14.

Together, the metabolomic and gene expression analyses highlight the heterogeneity of GBM cells both within individual tumors and across patients. These findings suggest that mesenchymal-like GBM cells exhibit higher metabolic activity compared to their NPC/OPC-like counterparts.

DISCUSSION

Our newly established cohort consists of 78 patients (34 women, 44 men), with an average age of approximately 60 years. Our cohort aligns with expected epidemiological characteristics[2], including: 1) a higher proportion of IDH-wt cases (77%) with ATRX status reflecting this distribution (83% WT); 2) IDH-wt GBM showing a higher Ki-67 proliferative index; and 3) half of the tumors exhibiting p53 overexpression and/or MGMT promoter hypermethylation. Recognizing the critical role of GSCs in the aggressiveness and therapy resistance of glioblastoma[19–21,27], we then focused our efforts on establishing new GSC lines derived from biopsies. By employing serum-free stem-cell optimized culture conditions, we are likely to better replicate GBM biology, as evidence indicates that patient-derived GSC lines in these conditions closely mirror patient's primary tumor[28]. Among our patient samples, we were able to characterize the percentage of GSCs using the sphere formation assay, with values ranging from 4% to 26%. The proportion of cells exhibiting stem cell-like properties, such as self-renewal, differentiation potential, and tumorigenicity, can vary significantly depending on factors like the tumor's origin, isolation method, and culture conditions[29–31]. GBM cells, particularly those with stem-like properties, also possess the ability to undergo metabolic reprogramming to meet the increased energy, lipid, protein, and sugar demands required for their growth, proliferation, and motility. This metabolic plasticity is essential for sustaining the self-renewal and tumorigenic potential of GSCs, highlighting the complex interplay between the stem cell-like characteristics of GBM cells and their metabolic needs for tumor progression.

GBM growth is primarily influenced by its microenvironment and is largely driven by glucose and glutamine metabolism, which supply energy and support anabolism[25,32]. Metabolism, signalling, and cellular functions are closely coordinated and regulated to maintain tumour homeostasis and therapy resistance[12]. Furthermore, GBM cancer cells are highly heterogeneous andreprogram their metabolism in diverse ways during tumor development, enabling them to support uncontrolled proliferation and survival under nutrient-deprived conditions[33]. This metabolic reprogramming, driven in part by the diversity of molecular alterations characterizing these tumors, enhances the biosynthesis of cellular building blocks, energy production, and redox balance[33,34]. A notable example of this phenomenon is the Warburg effect, a characteristic feature of cancer metabolism, which describes the shift in cancer cells toward increased glucose uptake, glycolysis, and lactate production, even in the presence of oxygen[35,36]. This metabolic shift possibly leads to high levels of glutamine, glutamate, aspartate, citrate, malate, lactate and nicotinamide, as seen in C38 and to a lesser extent in C15

and C39. Further analysis is needed to validate this observation. Glutamine utilization by cancer cells, through its conversion to glutamate and then α-ketoglutarate, can then enter the canonical TCA cycle as well as follows a counterclockwise direction to generate citrate[37]. An elevated concentration of nicotinamide, as present in C38, is also present in Warburg effect as pyruvate, derived from glycolysis, enters the mitochondria to produce new NADH, which, through the action of nicotinamide nucleotide transhydrogenase, can be converted to NADPH. This NADPH, through chemical kinetics, helps stimulate citrate production[38]. Overall, mitochondria in cancer cells process glutamine, glutamate, malate, and pyruvate, and export citrate, α-ketoglutarate, and aspartate into the cytoplasm where they are converted into metabolites necessary for cell growth[39]. This metabolic shift results in lactate production, causing acidification of the tumor microenvironment, which creates an immunosuppressive setting that promotes cancer cell growth and invasion[35,40,41]. Taken together, the Warburg effect supplies cancer cells with an abundance of glycolytic intermediates that serve as substrates for various biosynthetic pathways, including the production of nucleotides and amino acids, meeting the heightened demands of rapidly proliferating cells[39].

The serine-glycine and one-carbon metabolism pathway is another critical and complex metabolic network that plays a key role in tumorigenesis and therapy resistance[42]. Serine and glycine synthesis, critical for tumor growth and survival, involves two processes: the de novo synthesis of serine from glucose followed by it's conversion into glycine. These pathways enable nucleotide production, which is essential for DNA and RNA replication, thereby sustaining cell proliferation[34,43,44]**.** Beyond their roles in biosynthesis, serine and glycine are pivotal in maintaining cellular redox homeostasis[45]. They supply reductive equivalents, such as glutathione, which scavenges reactive oxygen species and mitigates oxidative stress. Furthermore, these metabolites regulate the methylation of DNA, RNA, and proteins, influencing gene expression, protein translation, and post-translational modifications that affect protein function and stability[45]. By integrating these diverse processes, serine and glycine play a central role in supporting tumor growth and ensuring survival of proneural cancer cells, such as C14, therefore these amino acids could be plausible therapeutic targets[46,47]. While lysine can serve as a biosynthetic molecule, energy source, and antioxidant, its pathological role in cancer remains poorly understood. A recent study demonstrated that a subtype of GSC can reprogram lysine catabolism by overexpressing the transporter SLC7A2, leading to an accumulation of lysine, as seen in C15[48]. Moreover, reducing lysine levels in tumor tissue resulted in improved survival and a decrease in tumor cell counts. The elevated levels of cysteine also observed in C15, and to

a lesser extent in C19, C38, and C39, can be attributed to the reaction of serine with a product of methionine degradation through the methyl cycle, resulting in the formation of cysteine and propionyl-CoA[49]. The latter then enters the TCA cycle though its conversion to succinyl-CoA.

There is now increasing research on the metabolic plasticity of GBM and efforts are being made to classify GSC based on their transcriptome[8,25]. A clear characterization based on both the metabolism and transcriptome is still lacking. To our knowledge, only one study has shown that mesenchymal GBM exhibits significantly higher glycolytic activity compared to proneural GBM[50]. By integrating metabolic characterization with the gene expression-based classification of GBM, vulnerabilities of each GBM can be pinpointed and personalized treatment options can be explored. The frequent genomic alterations of GBM adds a layer of complexity to the clinical diagnosis. While our study is mainly focused on glioblastoma cell lines, it would also be beneficial to explore the metabolome and transcriptome of astrocytoma and oligodendrocytoma cell lines. Indeed, the IDH1/2 mutation is a key genetic alteration in gliomas that significantly impacts their metabolism, as the resulting enzyme synthesizes the oncometabolite D-2-hydroxyglutarate (2HG) instead of α-ketoglutarate. This shift promotes a pro-methylation environment, contributing to aberrant DNA methylation[51]. In the context of p53 mutation, glioblastoma cells exhibit upregulation of enzymes involved in lipid metabolism, leading to an increase in cholesterol synthesis, as observed in C15 and C19, and this is associated with enhanced tumor growth[52–54]. Copy number alteration such as EGFR amplification, loss of chromosome 10q are also key modification which could impact both gene expression and metabolome. EGFR amplification, as found in C14 and C19, induces significant alterations in metabolic pathway such as glucose uptake, glycolysis, fatty acid synthesis, membrane lipid remodeling, cholesterol uptake, NAD+ production, and epigenetic modifications[54]. Loss of chromosome 10q, marked by *PTEN* loss in C14, C19, and C38, has been shown to promote aerobic glycolysis (the Warburg effect) in GBM by activating autophosphorylated PGK1[55]. Thus, the combination of multiple mutations in a GBM may create unique metabolic signatures that contribute to tumor progression, resistance to therapy, and disease outcomes, while also creating specific metabolic vulnerabilities that could be exploited for therapeutic purposes. Therefore, it is essential to conduct further studies to better understand how these mutations interact and how they drive metabolic reprogramming in GBM.

ACKNOWLEDGMENTS

The authors thank all the students and staff who assisted with sample collections at CHU de Québec – Université Laval, Hôpital de l'Enfant-Jésus, and especially the patients and their families for generously giving their time to participate in this study. This study was funded by the Canadian Cancer Society to MR (ID#1057382).

AUTHOR CONTRIBUTIONS

HLD: Conceptualization, Investigation, Formal Analysis, Methodology, Validation, Project administration, Writing—Review & Editing.
JM: Conceptualization, Investigation, Formal Analysis, Methodology, Validation, Writing—Review & Editing.
VF: Conceptualization, Methodology, Validation.
GK: Conceptualization, Methodology, Validation.
VW: Conceptualization, Methodology, Validation.
ML: Conceptualization, Methodology, Validation.
LB: Conceptualization, Methodology, Validation.
FR: Conceptualization, Methodology.
EB: Conceptualization, Methodology.
KM: Resources (recruitment of participants).
MD'A: Resources (recruitment of participants).
SS: Investigation.
MEH: Conceptualization, Validation, Project administration, Supervision
EAW: Investigation, Conceptualization, Formal Analysis, Conceptualization, Validation, Project administration, Writing—Review & Editing.
MR: Investigation, Conceptualization, Formal Analysis, Validation, Project administration, Funding acquisition, Supervision, Writing—original draft.
SMIH: Investigation, Conceptualization, Formal Analysis, Conceptualization, Validation, Project administration, Supervision, Writing—Review & Editing.

CONFLICTS OF INTEREST

The authors declare no conflicts of interest.

REFERENCES

1. Johnson, D.R.; O'Neill, B.P. Glioblastoma Survival in the United States before and during the Temozolomide Era. *J Neurooncol* **2012**, *107*, 359–364, doi:10.1007/s11060-011-0749-4.
2. Louis, D.N.; Perry, A.; Wesseling, P.; Brat, D.J.; Cree, I.A.; Figarella-Branger, D.; Hawkins, C.; Ng, H.K.; Pfister, S.M.; Reifenberger, G.; et al. The 2021 WHO Classification of Tumors of the Central Nervous System: A Summary. *Neuro Oncol* **2021**, *23*, 1231–1251, doi:10.1093/neuonc/noab106.
3. Stupp, R.; Hegi, M.E.; Mason, W.P.; van den Bent, M.J.; Taphoorn, M.J.B.; Janzer, R.C.; Ludwin, S.K.; Allgeier, A.; Fisher, B.; Belanger, K.; et al. Effects of Radiotherapy with Concomitant and Adjuvant Temozolomide versus Radiotherapy Alone on Survival in Glioblastoma in a Randomised Phase III Study: 5-Year Analysis of the EORTC-NCIC Trial. *Lancet Oncol* **2009**, *10*, 459–466, doi:10.1016/S1470-2045(09)70025-7.
4. Jiang, Y.; Uhrbom, L. On the Origin of Glioma. *Ups J Med Sci* **2012**, *117*, 113–121, doi:10.3109/03009734.2012.658976.
5. Ostrom, Q.T.; Bauchet, L.; Davis, F.G.; Deltour, I.; Fisher, J.L.; Langer, C.E.; Pekmezci, M.; Schwartzbaum, J.A.; Turner, M.C.; Walsh, K.M.; et al. The Epidemiology of Glioma in Adults: A "State of the Science" Review. *Neuro Oncol* **2014**, *16*, 896–913, doi:10.1093/neuonc/nou087.
6. Verhaak, R.G.W.; Hoadley, K.A.; Purdom, E.; Wang, V.; Qi, Y.; Wilkerson, M.D.; Miller, C.R.; Ding, L.; Golub, T.; Mesirov, J.P.; et al. Integrated Genomic Analysis Identifies Clinically Relevant Subtypes of Glioblastoma Characterized by Abnormalities in PDGFRA, IDH1, EGFR, and NF1. *Cancer Cell* **2010**, *17*, 98–110, doi:10.1016/j.ccr.2009.12.020.
7. Wang, Q.; Hu, B.; Hu, X.; Kim, H.; Squatrito, M.; Scarpace, L.; deCarvalho, A.C.; Lyu, S.; Li, P.; Li, Y.; et al. Tumor Evolution of Glioma-Intrinsic Gene Expression Subtypes Associates with Immunological Changes in the Microenvironment. *Cancer Cell* **2017**, *32*, 42-56.e6, doi:10.1016/j.ccell.2017.06.003.
8. Neftel, C.; Laffy, J.; Filbin, M.G.; Hara, T.; Shore, M.E.; Rahme, G.J.; Richman, A.R.; Silverbush, D.; Shaw, M.L.; Hebert, C.M.; et al. An Integrative Model of Cellular States, Plasticity, and Genetics for Glioblastoma. *Cell* **2019**, *178*, 835-849.e21, doi:10.1016/j.cell.2019.06.024.
9. Bernhard, C.; Reita, D.; Martin, S.; Entz-Werle, N.; Dontenwill, M. Glioblastoma Metabolism: Insights and Therapeutic Strategies. *International Journal of Molecular Sciences* **2023**, *24*, 9137, doi:10.3390/ijms24119137.
10. Garcia, J.H.; Jain, S.; Aghi, M.K. Metabolic Drivers of Invasion in Glioblastoma. *Front. Cell Dev. Biol.* **2021**, *9*, doi:10.3389/fcell.2021.683276.
11. Wolf, A.; Agnihotri, S.; Guha, A. Targeting Metabolic Remodeling in Glioblastoma Multiforme. *Oncotarget* **2010**, *1*, 552–562, doi:10.18632/oncotarget.190.
12. Zarzuela, L.; Durán, R.V.; Tomé, M. Metabolism and Signaling Crosstalk in Glioblastoma Progression and Therapy Resistance. *Molecular Oncology n/a*, doi:10.1002/1878-0261.13571.
13. Zhao, J.; Ma, X.; Gao, P.; Han, X.; Zhao, P.; Xie, F.; Liu, M. Advancing Glioblastoma Treatment by Targeting Metabolism. *Neoplasia* **2024**, *51*, 100985, doi:10.1016/j.neo.2024.100985.
14. Lee, J.; Kotliarova, S.; Kotliarov, Y.; Li, A.; Su, Q.; Donin, N.M.; Pastorino, S.; Purow, B.W.; Christopher, N.; Zhang, W.; et al. Tumor Stem Cells Derived from Glioblastomas Cultured in bFGF and EGF More Closely Mirror the Phenotype and Genotype of Primary Tumors than Do Serum-Cultured Cell Lines. *Cancer Cell* **2006**, *9*, 391–403, doi:10.1016/j.ccr.2006.03.030.
15. Xie, Y.; Bergström, T.; Jiang, Y.; Johansson, P.; Marinescu, V.D.; Lindberg, N.; Segerman, A.; Wicher, G.; Niklasson, M.; Baskaran, S.; et al. The Human Glioblastoma Cell Culture

Resource: Validated Cell Models Representing All Molecular Subtypes. *EBioMedicine* **2015**, *2*, 1351–1363, doi:10.1016/j.ebiom.2015.08.026.
16. Jacob, F.; Salinas, R.D.; Zhang, D.Y.; Nguyen, P.T.T.; Schnoll, J.G.; Wong, S.Z.H.; Thokala, R.; Sheikh, S.; Saxena, D.; Prokop, S.; et al. A Patient-Derived Glioblastoma Organoid Model and Biobank Recapitulates Inter- and Intra-Tumoral Heterogeneity. *Cell* **2020**, *180*, 188-204.e22, doi:10.1016/j.cell.2019.11.036.
17. Wu, M.; Wang, T.; Ji, N.; Lu, T.; Yuan, R.; Wu, L.; Zhang, J.; Li, M.; Cao, P.; Zhao, J.; et al. Multi-Omics and Pharmacological Characterization of Patient-Derived Glioma Cell Lines. *Nat Commun* **2024**, *15*, 6740, doi:10.1038/s41467-024-51214-y.
18. Kim, S.-C.; Cho, Y.-E.; Shin, Y.-K.; Yu, H.J.; Chowdhury, T.; Kim, S.; Yi, K.S.; Choi, C.-H.; Cha, S.-H.; Park, C.-K.; et al. Patient-Derived Glioblastoma Cell Lines with Conserved Genome Profiles of the Original Tissue. *Sci Data* **2023**, *10*, 448, doi:10.1038/s41597-023-02365-y.
19. Auffinger, B.; Spencer, D.; Pytel, P.; Ahmed, A.U.; Lesniak, M.S. The Role of Glioma Stem Cells in Chemotherapy Resistance and Glioblastoma Multiforme Recurrence. *Expert Rev Neurother* **2015**, *15*, 741–752, doi:10.1586/14737175.2015.1051968.
20. Heffernan, J.M.; Sirianni, R.W. Modeling Microenvironmental Regulation of Glioblastoma Stem Cells: A Biomaterials Perspective. *Frontiers in Materials* **2018**, *5*.
21. Roos, A.; Ding, Z.; Loftus, J.C.; Tran, N.L. Molecular and Microenvironmental Determinants of Glioma Stem-Like Cell Survival and Invasion. *Front Oncol* **2017**, *7*, 120, doi:10.3389/fonc.2017.00120.
22. Gonthier, K.; Poluri, R.T.K.; Weidmann, C.; Tadros, M.; Audet-Walsh, É. Reprogramming of Isocitrate Dehydrogenases Expression and Activity by the Androgen Receptor in Prostate Cancer. *Mol Cancer Res* **2019**, *17*, 1699–1709, doi:10.1158/1541-7786.MCR-19-0020.
23. Lafront, C.; Germain, L.; Campolina-Silva, G.H.; Weidmann, C.; Berthiaume, L.; Hovington, H.; Brisson, H.; Jobin, C.; Frégeau-Proulx, L.; Cotau, R.; et al. The Estrogen Signaling Pathway Reprograms Prostate Cancer Cell Metabolism and Supports Proliferation and Disease Progression. *J Clin Invest* **2024**, *134*, e170809, doi:10.1172/JCI170809.
24. Price, M.; Ballard, C.; Benedetti, J.; Neff, C.; Cioffi, G.; Waite, K.A.; Kruchko, C.; Barnholtz-Sloan, J.S.; Ostrom, Q.T. CBTRUS Statistical Report: Primary Brain and Other Central Nervous System Tumors Diagnosed in the United States in 2017–2021. *Neuro-Oncology* **2024**, *26*, vi1–vi85, doi:10.1093/neuonc/noae145.
25. De Silva, M.I.; Stringer, B.W.; Bardy, C. Neuronal and Tumourigenic Boundaries of Glioblastoma Plasticity. *Trends Cancer* **2023**, *9*, 223–236, doi:10.1016/j.trecan.2022.10.010.
26. Bhat, K.P.L.; Balasubramaniyan, V.; Vaillant, B.; Ezhilarasan, R.; Hummelink, K.; Hollingsworth, F.; Wani, K.; Heathcock, L.; James, J.D.; Goodman, L.D.; et al. Mesenchymal Differentiation Mediated by NF-κB Promotes Radiation Resistance in Glioblastoma. *Cancer Cell* **2013**, *24*, 331–346, doi:10.1016/j.ccr.2013.08.001.
27. Chen, J.; Li, Y.; Yu, T.-S.; McKay, R.M.; Burns, D.K.; Kernie, S.G.; Parada, L.F. A Restricted Cell Population Propagates Glioblastoma Growth after Chemotherapy. *Nature* **2012**, *488*, 522–526, doi:10.1038/nature11287.
28. Joo, K.M.; Kim, J.; Jin, J.; Kim, M.; Seol, H.J.; Muradov, J.; Yang, H.; Choi, Y.-L.; Park, W.-Y.; Kong, D.-S.; et al. Patient-Specific Orthotopic Glioblastoma Xenograft Models Recapitulate the Histopathology and Biology of Human Glioblastomas in Situ. *Cell Rep* **2013**, *3*, 260–273, doi:10.1016/j.celrep.2012.12.013.
29. Galli, R.; Binda, E.; Orfanelli, U.; Cipelletti, B.; Gritti, A.; De Vitis, S.; Fiocco, R.; Foroni, C.; Dimeco, F.; Vescovi, A. Isolation and Characterization of Tumorigenic, Stem-like Neural Precursors from Human Glioblastoma. *Cancer Res* **2004**, *64*, 7011–7021, doi:10.1158/0008-5472.CAN-04-1364.
30. Kanabur, P.; Guo, S.; Rodgers, C.M.; Simonds, G.R.; Kelly, D.F.; Gourdie, R.G.; Verbridge, S.S. Patient-Derived Glioblastoma Stem Cells Respond Differentially to Targeted Therapies. *Oncotarget* **2016**, *7*, 86406–86419, doi:10.18632/oncotarget.13415.

31. Knights, M.J.; Kyle, S.; Ismail, A. Characteristic Features of Stem Cells in Glioblastomas: From Cellular Biology to Genetics. *Brain Pathol* **2012**, *22*, 592–606, doi:10.1111/j.1750-3639.2012.00573.x.
32. Stadlbauer, A.; Zimmermann, M.; Doerfler, A.; Oberndorfer, S.; Buchfelder, M.; Coras, R.; Kitzwögerer, M.; Roessler, K. Intratumoral Heterogeneity of Oxygen Metabolism and Neovascularization Uncovers 2 Survival-Relevant Subgroups of IDH1 Wild-Type Glioblastoma. *Neuro Oncol* **2018**, *20*, 1536–1546, doi:10.1093/neuonc/noy066.
33. Hanahan, D.; Weinberg, R.A. Hallmarks of Cancer: The next Generation. *Cell* **2011**, *144*, 646–674, doi:10.1016/j.cell.2011.02.013.
34. DeBerardinis, R.J. Serine Metabolism: Some Tumors Take the Road Less Traveled. *Cell Metab* **2011**, *14*, 285–286, doi:10.1016/j.cmet.2011.08.004.
35. Vander Heiden, M.G.; Cantley, L.C.; Thompson, C.B. Understanding the Warburg Effect: The Metabolic Requirements of Cell Proliferation. *Science* **2009**, *324*, 1029–1033, doi:10.1126/science.1160809.
36. DeBerardinis, R.J.; Chandel, N.S. We Need to Talk about the Warburg Effect. *Nat Metab* **2020**, *2*, 127–129, doi:10.1038/s42255-020-0172-2.
37. Gaglio, D.; Metallo, C.M.; Gameiro, P.A.; Hiller, K.; Danna, L.S.; Balestrieri, C.; Alberghina, L.; Stephanopoulos, G.; Chiaradonna, F. Oncogenic K-Ras Decouples Glucose and Glutamine Metabolism to Support Cancer Cell Growth. *Mol Syst Biol* **2011**, *7*, 523, doi:10.1038/msb.2011.56.
38. Xie, T.; Chen, M.; Nielsen, J.; Xia, J. Multi-Omics Analyses of the Transition to the Crabtree Effect in S. Cerevisiae Reveals a Key Role for the Citric Acid Shuttle. *FEMS Yeast Res* **2022**, *22*, foac030, doi:10.1093/femsyr/foac030.
39. Alberghina, L. The Warburg Effect Explained: Integration of Enhanced Glycolysis with Heterogeneous Mitochondria to Promote Cancer Cell Proliferation. *Int J Mol Sci* **2023**, *24*, 15787, doi:10.3390/ijms242115787.
40. Colen, C.B.; Shen, Y.; Ghoddoussi, F.; Yu, P.; Francis, T.B.; Koch, B.J.; Monterey, M.D.; Galloway, M.P.; Sloan, A.E.; Mathupala, S.P. Metabolic Targeting of Lactate Efflux by Malignant Glioma Inhibits Invasiveness and Induces Necrosis: An in Vivo Study. *Neoplasia* **2011**, *13*, 620–632, doi:10.1593/neo.11134.
41. Chen, S.; Xu, Y.; Zhuo, W.; Zhang, L. The Emerging Role of Lactate in Tumor Microenvironment and Its Clinical Relevance. *Cancer Letters* **2024**, *590*, 216837, doi:10.1016/j.canlet.2024.216837.
42. Reina-Campos, M.; Diaz-Meco, M.T.; Moscat, J. The Complexity of the Serine Glycine One-Carbon Pathway in Cancer. *Journal of Cell Biology* **2019**, *219*, e201907022, doi:10.1083/jcb.201907022.
43. Geeraerts, S.L.; Heylen, E.; De Keersmaecker, K.; Kampen, K.R. The Ins and Outs of Serine and Glycine Metabolism in Cancer. *Nat Metab* **2021**, *3*, 131–141, doi:10.1038/s42255-020-00329-9.
44. Possemato, R.; Marks, K.M.; Shaul, Y.D.; Pacold, M.E.; Kim, D.; Birsoy, K.; Sethumadhavan, S.; Woo, H.-K.; Jang, H.G.; Jha, A.K.; et al. Functional Genomics Reveal That the Serine Synthesis Pathway Is Essential in Breast Cancer. *Nature* **2011**, *476*, 346–350, doi:10.1038/nature10350.
45. Locasale, J.W. Serine, Glycine and the One-Carbon Cycle: Cancer Metabolism in Full Circle. *Nat Rev Cancer* **2013**, *13*, 572–583, doi:10.1038/nrc3557.
46. Engel, A.L.; Lorenz, N.I.; Klann, K.; Münch, C.; Depner, C.; Steinbach, J.P.; Ronellenfitsch, M.W.; Luger, A.-L. Serine-Dependent Redox Homeostasis Regulates Glioblastoma Cell Survival. *Br J Cancer* **2020**, *122*, 1391–1398, doi:10.1038/s41416-020-0794-x.
47. Seliger, C.; Rauer, L.; Wüster, A.-L.; Moeckel, S.; Leidgens, V.; Jachnik, B.; Ammer, L.-M.; Heckscher, S.; Dettmer, K.; Riemenschneider, M.J.; et al. Heterogeneity of Amino Acid Profiles

of Proneural and Mesenchymal Brain-Tumor Initiating Cells. *Int J Mol Sci* **2023**, *24*, 3199, doi:10.3390/ijms24043199.
48. Gül, D.; Krämer, O.H.; Reinhardt, C. Starving out Brain Tumors: A Reprogrammed Lysine Catabolism Serves as a Novel Target for Glioblastoma Treatment. *Sig Transduct Target Ther* **2023**, *8*, 1–3, doi:10.1038/s41392-023-01616-z.
49. Pelley, J.W. 12 - Amino Acid and Heme Metabolism. In *Elsevier's Integrated Review Biochemistry (Second Edition)*; Pelley, J.W., Ed.; W.B. Saunders: Philadelphia, 2012; pp. 99–107 ISBN 978-0-323-07446-9.
50. Mao, P.; Joshi, K.; Li, J.; Kim, S.-H.; Li, P.; Santana-Santos, L.; Luthra, S.; Chandran, U.R.; Benos, P.V.; Smith, L.; et al. Mesenchymal Glioma Stem Cells Are Maintained by Activated Glycolytic Metabolism Involving Aldehyde Dehydrogenase 1A3. *Proc Natl Acad Sci U S A* **2013**, *110*, 8644–8649, doi:10.1073/pnas.1221478110.
51. M Gagné, L.; Boulay, K.; Topisirovic, I.; Huot, M.-É.; Mallette, F.A. Oncogenic Activities of IDH1/2 Mutations: From Epigenetics to Cellular Signaling. *Trends Cell Biol* **2017**, *27*, 738–752, doi:10.1016/j.tcb.2017.06.002.
52. Loughran, R.; Emerling, B.M. Mechanistic Roles of Mutant P53 Governing Lipid Metabolism. *Adv Biol Regul* **2022**, *83*, 100839, doi:10.1016/j.jbior.2021.100839.
53. Pirmoradi, L.; Seyfizadeh, N.; Ghavami, S.; Zeki, A.A.; Shojaei, S. Targeting Cholesterol Metabolism in Glioblastoma: A New Therapeutic Approach in Cancer Therapy. *Journal of Investigative Medicine* **2019**, *67*, 715–719, doi:10.1136/jim-2018-000962.
54. Bi, J.; Khan, A.; Tang, J.; Armando, A.M.; Wu, S.; Zhang, W.; Gimple, R.C.; Reed, A.; Jing, H.; Koga, T.; et al. Targeting Glioblastoma Signaling and Metabolism with a Re-Purposed Brain-Penetrant Drug. *Cell Rep* **2021**, *37*, 109957, doi:10.1016/j.celrep.2021.109957.
55. Qian, X.; Li, X.; Shi, Z.; Xia, Y.; Cai, Q.; Xu, D.; Tan, L.; Du, L.; Zheng, Y.; Zhao, D.; et al. PTEN Suppresses Glycolysis by Dephosphorylating and Inhibiting Autophosphorylated PGK1. *Mol Cell* **2019**, *76*, 516-527.e7, doi:10.1016/j.molcel.2019.08.006.

TABLE

Table 1. Characteristics of qPCR primer pairs. *Abbreviations:* MES, mesenchymal; MES-Trans, mesenchymal transition; NPC, neural progenitor cell; OPC, oligodendrocyte progenitor cell.

Group	*Gene*	Forward primer	Reverse primer	Binding efficiency
MES-like	*ANXA1*	TGCAAGAAGGTAGAGATAAAGACAC	TCACAGTTTGAACATATTCCTGCTC	1,087
MES-like	*CHI3L1*	CCATCACAGTCCCCTGTTCC	CCATCACCAGCTTACTGGCA	1,14
MES-like	*CD44*	CTGTACACCCCATCCCAGAC	CTTGCCTCTTGGTTGCTGTC	1,019
NPC-like	*DLL3*	GCTCGAGGACGAATGTGAGG	TCTAGGCATCGGCATTCACC	0,999
OPC-like	*OLIG2*	ATAGATCGACGCGACACCAGC	TCCCTCGGACCCGAAAATCTG	0,994
MES-Trans	*SNAI2*	CGTAAAGGAGCCGGGTGACT	GACACGGCGGTCCCTACAG	1,007
MES-Trans	*TGFB1*	GTGGACATCAACGGGTTCAC	ATGAGAAGCAGGAAAGGCCG	0,919

FIGURE

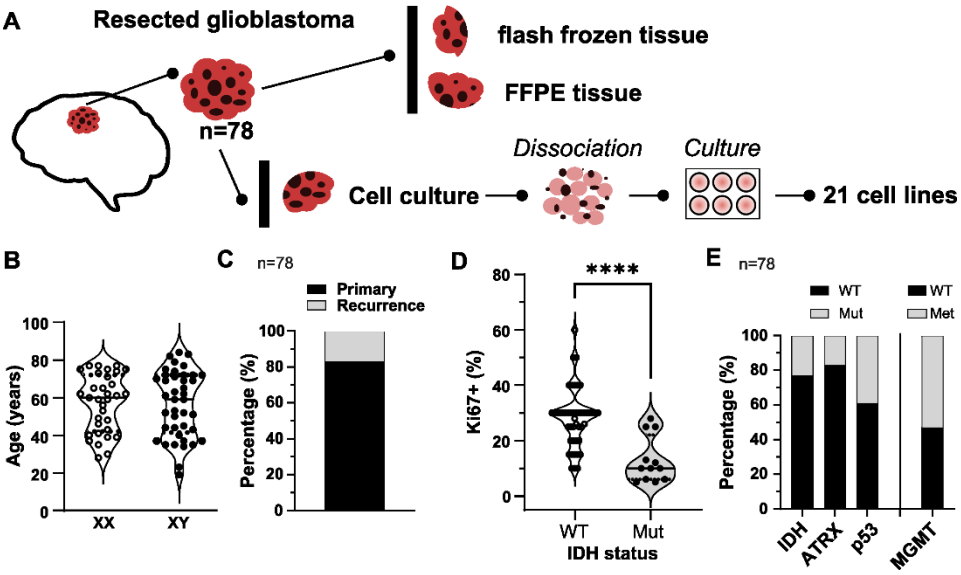

Figure 1. A. Generation of the glioblastoma biobank from resected human tissue. **B.** Biopsies came from 34 women and 44 men with a similar age (Women, median=60 years old; Men, median=59 years old). **C.** Biopsies mostly came from a primary resection. **D.** Percentage of Ki67-positive cells within the biopsy compared to IDH status. **E.** Percentage within our biobank of biopsies with WT or Mut status. **D.** Most of the biopsies are IDH (77%), ATRX (83%) and p53 (61%) WT. Half of the biopsy are MGMT WT. Mutated IDH biopsies are usually not tested for MGMT status. *Statistical analysis:* C. unpaired t-test. *Abbreviations:* ATRX, X-linked nuclear protein; FFPE, Formalin-Fixed Paraffin-Embedded; IDH, isocitrate dehydrogenase; n, number; MGMT, O^6-methylguanine-DNA methyltransferase; Mut, mutated; p53, tumor protein 53; WT, wild-type.

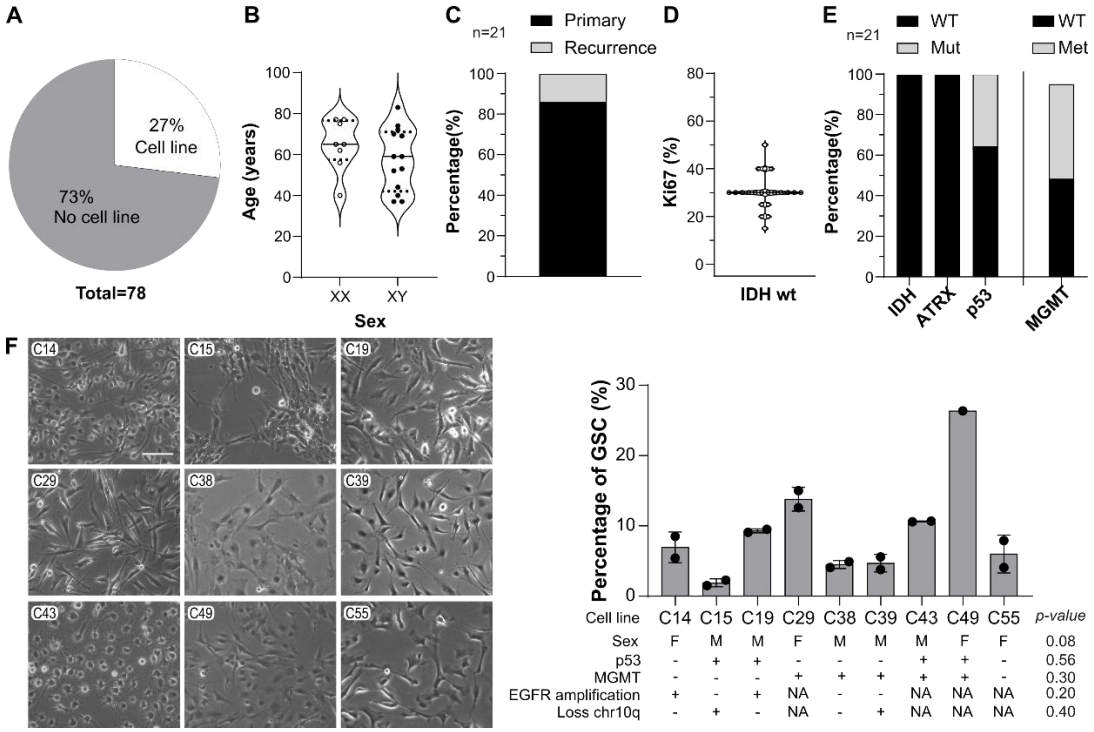

Figure 2. A. Out of 78 GBM, 27% gave cell lines. **B.** Cell lines came from 8 women and 13 men with a similar age (Women, median=65 years old; Men, median=58 years old). **C.** Cell lines mostly came from a primary resection. **D.** Percentage of Ki67-positive cells within the biopsy compared to IDH status. All our cell lines are IDH and ATRX WT. **E.** Percentage within our cell lines with WT or Mut/Met status: 62% and 38% of the cell lines are p53 and MGMT WT respectively. **F.** Representative picture of 9 GSC cell lines to be used in the downstream experiments. Using limiting dilution assay, we assessed the percentage of GSCs within the 9 cell lines. No correlations have been found between GSC percentage and sex, p53, MGMT, EGFR amplification, loss of the chromosome 10q status. *Scale bar:* 100μm. *Statistical analysis:* **F**, Unpaired t-test or Mann-Whitney test. *Abbreviations:* ATRX, X-linked nuclear protein; EGFR, epidermal growth factor receptor; IDH, isocitrate dehydrogenase; Loss chr10q, loss of the chromosome 10q; MGMT, O^6-methylguanine-DNA methyltransferase; Mut, mutated; p53, tumor protein 53; WT, wild-type.

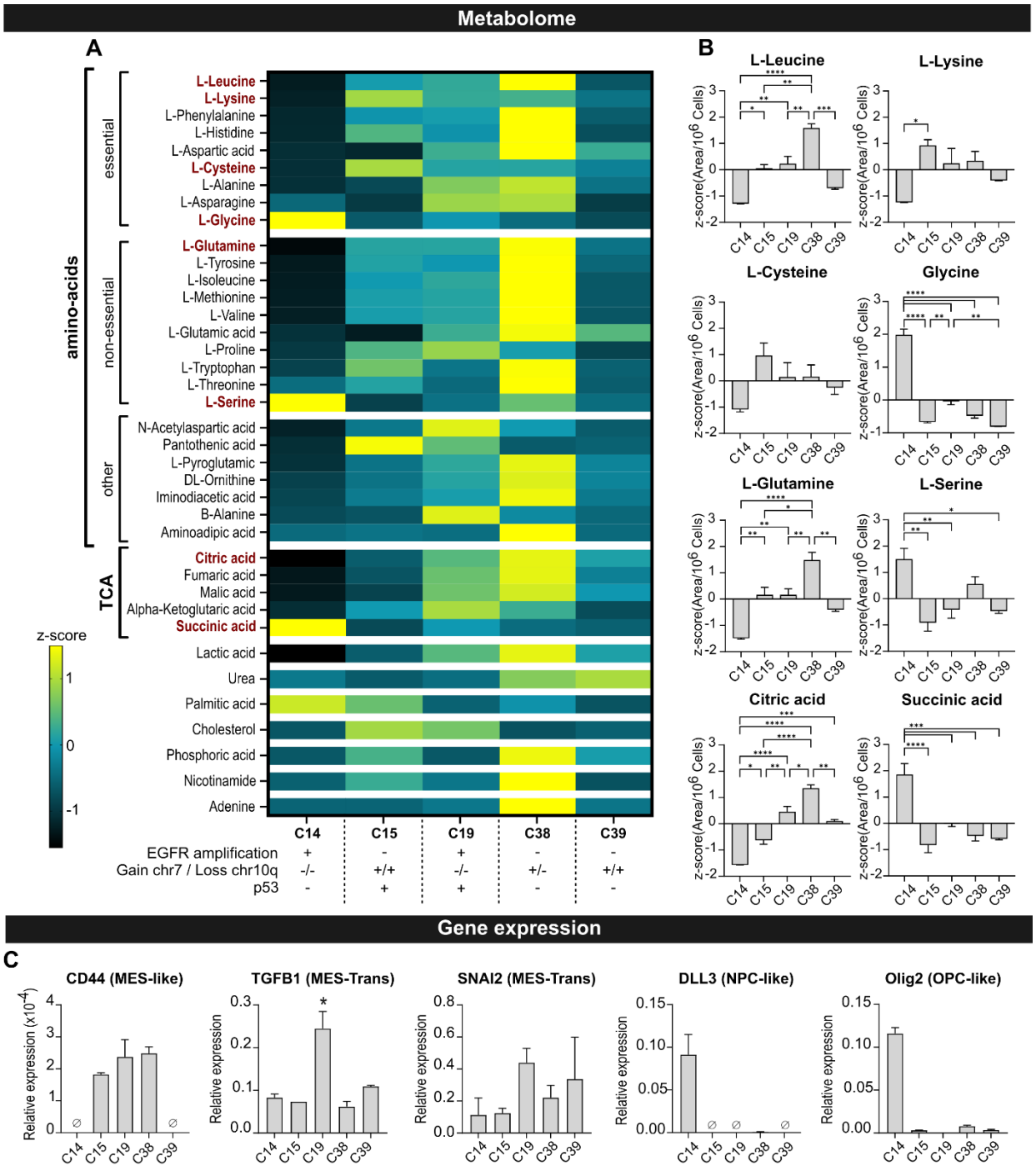

Figure 3. A. Metabolomic assay was performed on five selected cell lines. **B.** Differences between essential amino-acids, non-essential amino-acids, subtract derived from TCA cycle, and fatty acids levels were compared. **C.** Characterisation of RNA levels specific to mesynchymal (CD44), mesenchymal transition (TGFB1, SNAI2), NPC-like (DLL3) or OPC-like (Olig2) GBM cell type using RTq-PCR. *Statistical analysis:* (**A**) Mean of 3 independent replicates; (**B**) 3 independent replicates; (**C**) 2 independent replicates; (**B-C**) one-way Anova followed by Tukey's multiple comparisons test was performed or Kruskal-Wallis test followed by Dunn's multiple comparisons test. *Abbreviations:* EGFR, epidermal growth factor receptor; Gain chr7, trisomy of chromosome

7; Loss chr10q, loss of the chromosome 10q; MES, mesenchymal; MES-Trans, mesenchymal transition; Mut, mutated; NPC, neural progenitor cell; OPC, oligodendrocyte progenitor cell; p53, tumor protein 53; WT, wild-type.